THE JOURNAL OF PHYSICAL CHEMISTRY B
A JOURNAL OF THE AMERICAN CHEMICAL SOCIETY

pubs.acs.org/JPCB

Article

Red-Purple Photochromic Indigos from Green Chemistry: Mono-*t*BOC or Di-*t*BOC *N*-Substituted Indigos Displaying Excited State Proton Transfer or Photoisomerization

Daniela Pinheiro, Adelino M. Galvão, Marta Pineiro, and J. Sérgio Seixas de Melo*

Cite This: *J. Phys. Chem. B* 2021, 125, 4108–4119

Read Online

ACCESS | Metrics & More | Article Recommendations | Supporting Information

ABSTRACT: In indigo, excited state proton transfer (ESPT) is known to be associated with the molecular mechanism responsible for highly efficient radiationless deactivation. When this route is blocked (partially or totally), new deactivation routes become available. Using new green chemistry procedures, with favorable green chemistry metrics, monosubstitution and disubstitution of N group(s) in indigo, by *tert*-butoxy carbonyl groups, *N*-(*tert*-butoxycarbonyl)indigo (NtBOCInd) and *N,N′*-(*tert*-butoxycarbonyl)indigo (N,N'tBOCInd), respectively, were synthetically accomplished. The compounds display red to purple colors depending on the solvent and substitution. Different excited-state deactivation pathways were observed and found to be structure- and solvent-dependent. *Trans*−*cis* photoisomerization was found to be absent with NtBOCInd and present with N,N'tBOCInd in nonpolar solvents. Time-resolved fluorescence experiments revealed single-exponential decays for the two compounds which, linked to time-dependent density functional theory (TDDFT) studies, show that with NtBOCInd ESPT is extremely fast and barrierless—predicted to be 1 kJ mol^{-1} in methylcyclohexane and 5 kJ mol^{-1} in dimethylsulfoxide—, which contrasts with ∼11 kJ mol^{-1} experimentally obtained for indigo. An alternative ESPT, competitive with the N−H···O═C intramolecular pathway, involving dimer units is also probed by TDDFT and found to be consistent with the experimentally observed time-resolved data. N,N'tBOCInd, where ESPT is precluded, shows solvent-dependent *trans*−*cis*/*cis*−*trans* photoisomerization and is surprisingly found to be more stable in the nonemissive *cis* conformation, whose deactivation to S_0 is found to be solvent-dependent.

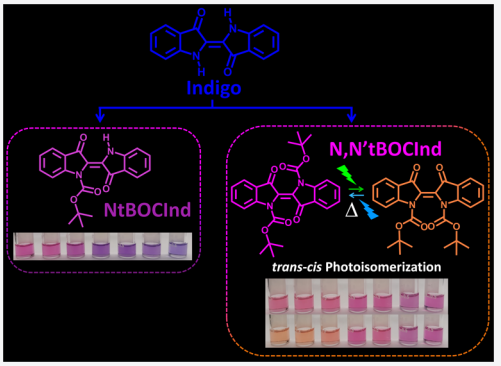

1. INTRODUCTION

In recent years, photochromic molecules have witnessed new exciting developments, with particular emphasis on photoswitchable systems with broad applications in different scientific domains.[1−3] Photochromic materials undergo light-induced reversible change of color.[4] The spectroscopy and photochemistry of indigo had its pioneering studies during the 1950s to 1990s period where it was concluded that, in contrast to indigo,[5] indigo derivatives, such as thioindigo,[6−9] oxindigo,[10] selenoindigo,[11,12] *N,N′*-substituted indigo[3,5,13−19] and hemi-indigo photochroms,[20] undergo *trans*−*cis* photoisomerization. Although this isomerization process was present in some of these compounds, there was a lack, until very recently, of real interest in the use of these molecules for photochromic applications, in part because of their poor solubility and low photoisomerization quantum yields. This does not occur with the reduced indigo derivatives, where, for example, leuco indigo can have a photochemistry quantum yield (for the *trans* to *cis* conversion) of 90%[21] and also with some *N,N′*-substituted indigo derivatives.[13−15,22,23] Without question, *trans*−*cis* photoisomerization is considered a fundamental chemical reaction with great technological interest and many and diversified applications in photoresponsive systems.[15,24−26]

Trans−*cis* photoisomerizable compounds can convert light energy into mechanical work and therefore display a large variety of applications including optical data storage,[27] photoactuating polymeric materials, photoswitchable optical elements, and permeation membranes.[28] In the context of biomedical applications, photoswitches have become a key tool to remotely and noninvasively regulate processes in vivo, for example, in photopharmacology,[29−31] super-resolution fluorescence imaging,[32] and optochemical genetics.[3,33] Photochromic indigo derivatives seem to have gained renewed interest, not only because of the high photochemistry quantum yields that can be obtained, but also because of the high stability that some of these compounds possess.[34,35]

Received: January 6, 2021
Revised: March 26, 2021
Published: April 14, 2021

Downloaded via UNIVERSIDADE DE COIMBRA 00500 on July 13, 2023 at 09:06:03 (UTC).
See https://pubs.acs.org/sharingguidelines for options on how to legitimately share published articles.

ACS Publications
© 2021 American Chemical Society

https://doi.org/10.1021/acs.jpcb.1c00120
J. Phys. Chem. B 2021, 125, 4108–4119

In this work, mono- and disubstituted indigos with a *tert*-butoxy carbonyl (tBOC) group, *N*-(*tert*-butoxycarbonyl)indigo (NtBOCInd) and *N,N′*-di(*tert*-butoxycarbonyl)indigo (N,N'tBOCInd), respectively, see Chart 1, were synthetized

Chart 1. Structures and Acronyms of NtBOCInd and N,N'tBOCInd.

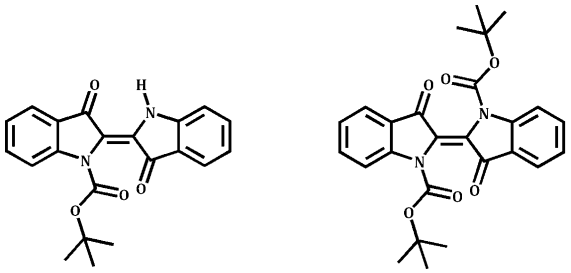

N-(*tert*-butoxycarbonyl)indigo (NtBOCInd)

N,N′-di(*tert*-butoxycarbonyl)indigo (N,N'tBOCInd)

following a new synthetic methodology with green chemistry procedures.[34] Comprehensive characterization of the excited-state deactivation processes of these two derivatives has been performed bearing in mind two fundamental research questions: (i) the facility of photoisomerization of N,N'tBOCInd as a highly competitive pathway for the excited-state deactivation and (ii) competition of this process with excited state proton transfer, ESPT, with NtBOCInd. The observed behavior could only be properly rationalized with density functional theory (DFT) and time-dependent density functional theory (TDDFT) calculations.

2. EXPERIMENTAL SECTION

2.1. General Synthetic Procedure for NtBOCInd and N,N'tBOCInd Derivatives. In a thick-glass microwave (MW) reactor, with a magnetic stirring bar, indigo (200 mg, 1 equiv) and sodium hydride, NaH (2 equiv), were dissolved in 1 mL of *N,N′*-dimethylformamide (DMF). Di-*tert*-butyl dicarbonate (4 equiv) and DMF was added to a total volume of 2 mL. The resulting mixture was heated under MW irradiation at 50 °C for 15 min. After cooling down to room temperature, the reaction mixture was extracted with dichloromethane and water, and the organic layer was dried overnight with anhydrous sodium sulfate. After this, the mixture was filtered, and the solvent was concentrated under reduced pressure. The crude product was purified by column chromatography (SiO_2) using ethyl acetate/hexane (1:3; v/v) as the eluent to yield NtBOCInd as a purple solid (82 mg and 30% yield) and N,N'tBOCInd as a red solid (116 mg and 33% yield).

The molecular structures of NtBOCInd and N,N'tBOCInd were confirmed by ^{1}H and ^{13}C nuclear magnetic resonance (NMR) spectroscopy and by gas chromatography−mass spectrometry (GC−MS) and/or high-resolution mass spectrometry (HRMS). Detailed information on the ^{1}H and ^{13}C NMR spectroscopy, GC−MS, and/or HRMS characterization is given in the SI.

2.2. Materials. Indigo (95%), sodium hydride (60% dispersion in mineral oil stored in a dry box), di-*tert*-butyl dicarbonate, and the reagents used in the ferrioxalate actinometer (potassium ferrioxalate, 1,10-phenanthroline, and sodium acetate) were obtained from commercial sources. All reagents used for the synthesis of the compounds were used without further purification. For the synthetic procedures, the solvents were of commercial pro analysis grade. For the spectral and photophysical determinations, the solvents used were of spectroscopic or equivalent grade.

2.3. Equipment and Methods. MW-assisted reactions were performed in a CEM Discover S-Class single-mode MW reactor, featuring continuous temperature and pressure and MW power monitoring.

Analytical thin-layer chromatography was performed on Macherey-Nagel ALUGRAM Xtra silica gel plates with a UV_{254} indicator. Visualization was accomplished using an ultraviolet lamp. A chromatography column was used with silica gel (230−400 mesh).

NMR spectra were recorded at room temperature in deuterated chloroform ($CDCl_3$) solutions on a Bruker Avance III spectrometer and a Bruker DRX-400 spectrometer, both operating at 400.13 MHz for ^{1}H and 100.61 MHz for ^{13}C, and are given in Figure SI1−4 in the SI. Chemical shifts for ^{1}H and ^{13}C are expressed in ppm, relatively to an internal standard of tetramethylsilane. Chemical shifts (δ) and coupling constants (J) are indicated in ppm and Hz, respectively.

GC−MS analyses were performed on a Hewlett-Packard 5973 MSD spectrometer, using electron ionization (70 eV), coupled with a Hewlett-Packard Agilent 6890 chromatography system, equipped with a HP-5 MS column (30 m × 0.25 mm × 0.25 μm) and high-purity helium as carrier gas. The initial temperature of 70 °C was increased to 250 °C at a 15 °C min^{-1} rate and held for 10 min. Then the temperature was increased to 290 °C at a 5 °C min^{-1} rate and held for 2 min, giving a total run time of 32 min. The flow of the carrier gas was maintained at 1.33 mL min^{-1}. The injector port was set at 250 °C.

HRMS was performed on a Bruker microTOF-Focus mass spectrometer equipped with an electrospray ionization time-of-flight source, the mass spectra are given in Figure SI5−6 in the SI. Absorption and fluorescence spectra were recorded on Cary 5000 UV−vis−NIR and Horiba Fluoromax 4 (or Fluorolog 3.22) spectrometers, respectively. Fluorescence spectra were corrected for the wavelength response of the system.

The fluorescence quantum yields (ϕ_F) at room temperature (T = 293 K) for NtBOCInd and N,N'tBOCInd in the different solvents were obtained by the comparative method (Eq. 1) using indigo in DMF (ϕ_F = 0.0023)[36] as the standard:

$$\phi_F^{cp} = \frac{\int I(\lambda)^{cp} d\lambda}{\int I(\lambda)^{ref} d\lambda} \times \frac{n_{cp}^2}{n_{ref}^2} \times \phi_F^{ref} \quad (1)$$

where $\int I(\lambda)^{cp} d\lambda$ is the integrated area under the emission spectra of the compound (cp) solutions and $\int I(\lambda)^{ref} d\lambda$ of the reference (ref) solution, n_{cp}^2 and n_{ref}^2 are the refractive index of the solvents in which the compounds and the reference were, respectively, dissolved, and ϕ_F^{ref} is the fluorescence quantum yield of the standard.

Fluorescence quantum yields at T = 77 K were obtained by comparison with the spectrum at T = 293 K run under the same experimental conditions using eq 2,

$$\phi_F^{77\ K} = \frac{\int I(\lambda)^{77\ K} d\lambda}{\int I(\lambda)^{293\ K} d\lambda} \times \phi_F^{293\ K} \times f_c \quad (2)$$

where $\int I(\lambda)^{x} d\lambda$ is the integrated area under the emission of the compound x = 77 and 293 K, $\phi_F^{293\ K}$ is the fluorescence quantum yield at 293 K, and f_c is the factor that considers the

https://doi.org/10.1021/acs.jpcb.1c00120
J. Phys. Chem. B 2021, 125, 4108−4119

"shrinkage" of the solvent (volume) upon cooling, given by $V_{77\ K}/V_{293\ K}$ (for 2-methyltetrahydofuran, it is assumed that f_c = 0.8).[37]

Fluorescence decays were measured using a home-built picosecond time-correlated single photon counting (ps-TCSPC) apparatus described elsewhere.[38] The excitation source consists of a tunable picosecond Spectra-Physics mode-lock Tsunami laser (Ti:sapphire) model 3950 (80 MHz repetition rate and tuning range 700−1000 nm), pumped by a 532 nm continuous wave Spectra-Physics Millennia Pro-10s laser. The excitation wavelength (λ_{exc} = 433 nm) was obtained with a Spectra-Physics harmonic generator, model GWU-23PS. To eliminate stray light from the light source, an RG530 filter was placed between the sample holder and the emission monochromator. The fluorescence decay curves were deconvoluted using the experimental instrument response function signal collected with a scattering solution (aqueous Ludox solution). The deconvolution procedure was performed using the modulation function method, as implemented by G. Striker in the SAND program, and previously reported in the literature.[39]

Irradiation with monochromatic light was carried out, at room temperature, with a xenon lamp (150 W). Photoisomerizations were performed with a FluoroMax-4 spectrophotometer with irradiation at 575 nm for NtBOCInd and for N,N'tBOCInd with irradiation at 560 nm for the *trans*−*cis* photoisomerization and at 416 nm for the *cis*−*trans* photoisomerization. In the experiments, the UV−vis absorption spectra were recorded with Ocean Optics USB2000 equipment. Samples were continuously stirred during the irradiation measurements to avoid the formation of concentration gradients of the photoproduct along the optical path. The photon flux for a system with monochromatic light and a specific geometry is calculated by actinometry. The most commonly used actinometer involves aqueous solutions of potassium ferrioxalate.[40] The moles of photons absorbed by the irradiated solution per second, I_{abs}, were obtained by the use of this actinometer. Detailed information of the use of the ferrioxalate actinometer and the determination of I_{abs} is given in the SI.

All theoretical calculations were of the DFT type and carried out using GAMESS-US version R3.[41] A range-corrected LC-BPBE (ω = 0.2 au^{-1}) functional, as implemented in GAMESS-US,[41] was used in both ground- and excited-state calculations. TDDFT calculations, with similar functionals, were used to probe the excited-state potential energy surface (PES). A solvent was included using the polarizable continuum model with the solvation model density to add corrections for cavitation, dispersion, and solvent structure. In the TDDFT calculation of Franck−Condon excitations, the dielectric constant of the solvent was split into a "bulk" component and a fast component, which is essentially the square of the refractive index. Under "adiabatic" conditions, only the static dielectric constant was used. In DFT or TDDFT calculations, a 6-31G** basis set was used.[41]

3. RESULTS AND DISCUSSION

3.1. Synthesis. Synthesis of NtBOCInd and N,N'tBOCInd, from indigo with sodium hydride (NaH) and di-*tert*-butyl dicarbonate in DMF,[34] Scheme SI1, was performed under MW irradiation with a continuous monitoring of power, temperature, and pressure. This allowed obtaining, with moderate yields, both products in only a few minutes (NtBOCInd, 30% and N,N'tBOCInd, 33% yields). Under MW irradiation conditions, the amount of solvent necessary to perform the reaction is strongly reduced, and the reaction time decreased when compared to conventional reaction procedures.[3,13,42−44] Compared with previously reported synthesis in which large amounts of solvents and long reaction times—hours or even days—are required to obtain N,N'tBOCInd, the developed methodology has favorable values of green chemistry metrics. Elimination of the solvent together with reduction of the mass of waste allows decreasing the E-factor[45] value to 8.3, comparing favorably with values obtained for classic methodologies 11.8[46] and 171.4[23] (Table SI1). To complete this mass-based metric, EcoScale was determined. EcoScale is a postsynthetic metric that takes into consideration price, safety, reaction operation conditions, and isolation and purification steps.[47,48] The MW-assisted methodology reaches an EcoScale value of 7.3, which is comparable with 18.5 and 7.7 values obtained for the referred conventional methods[23,46] (Table SI2).

3.2. Excited-State Characterization. *3.2.1. TDDFT and Experimental Absorption and Steady State Fluorescence Spectral Data.* Measurements of absorption, fluorescence emission, and excitation spectra of NtBOCInd and N,N'tBOCInd were conducted in seven solvents with different polarity (given here by the dielectric constant, ε') and viscosities (η) at room (T = 293 K) and low (T = 77 K) temperatures.

Indigo's color is known to be sensitive to solvent varying from red to blue.[49−52] Solutions of NtBOCInd and N,N'tBOCInd in the seven solvents, *n*-dodecane, methylcyclohexane (MCH), 2-methyltetrahydrofuran (2MeTHF), ethanol (EtOH), methanol (MeOH), DMF, and dimethylsulfoxide (DMSO), are depicted in Figure 1, showing the, solvent-dependent, palette of colors, from pale red to deep purple, passing through pink, more noticeably solvent-polarity-dependent for NtBOCInd.

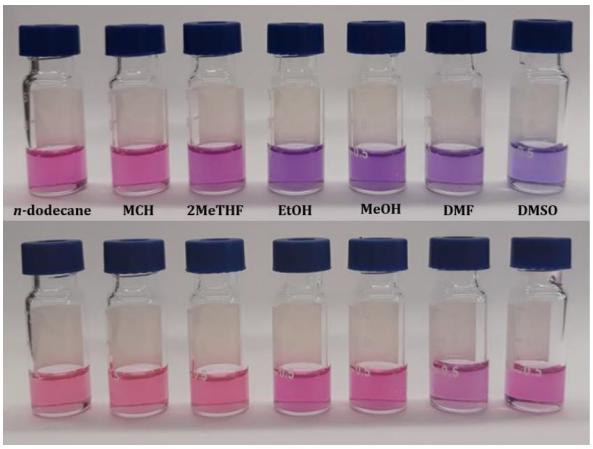

Figure 1. Picture of NtBOCInd (top) and N,N'tBOCInd (bottom) in *n*-dodecane, MCH, 2MeTHF, EtOH, MeOH, DMF, and DMSO at T = 293 K.

Figure 2 depicts the absorption, fluorescence emission, and excitation spectra of NtBOCInd and N,N'tBOCInd at T = 293 K, and Tables 1 and 2 display the spectral and photophysical data. NtBOCInd is blue-shifted by ca. ∼40 nm relative to indigo, and in N,N'tBOCInd, the blueshift is even more pronounced (53 nm in 2MeTHF, 59 nm in DMF and 67 nm in DMSO).

https://doi.org/10.1021/acs.jpcb.1c00120
J. Phys. Chem. B 2021, 125, 4108−4119

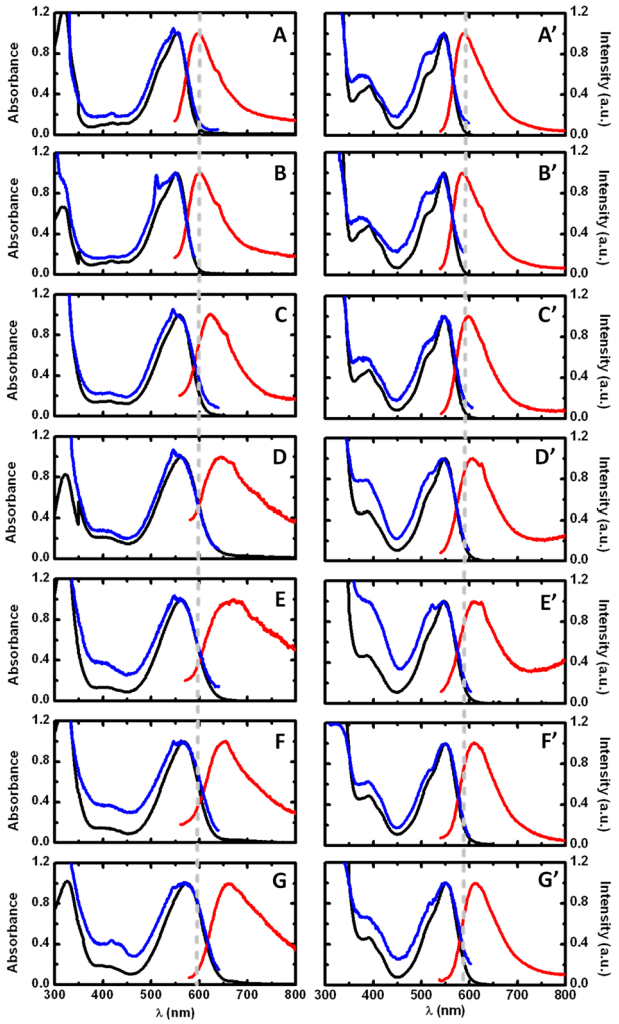

Figure 2. Normalized absorption (black line), excitation (blue line), and fluorescence emission (red line) spectra of NtBOCInd (left, A–G) and N,N'tBOCInd (right, A'–G') in *n*-dodecane (A,A'), MCH (B,B'), 2MeTHF(C), EtOH (D,D'), MeOH (E,E'), DMF (F,F'), and DMSO (G,G') solutions at T = 293 K. The emission spectra were obtained for NtBOCInd with λ_{exc} = 550–570 nm and the excitation spectra with λ_{em} = 600–650 nm, whereas for N,N'tBOCInd, the emission spectra were obtained with λ_{exc} = 530 nm and the excitation spectra with λ_{em} = 608–670 nm. The dashed vertical lines are meant to be guidelines to the eye.

Figure 3 (for N,N'tBOCInd) and Figure SI7 (for Indigo) map the orbital contours of the highest occupied molecular orbital (HOMO) and lowest unoccupied molecular orbital (LUMO) showing that the π system of the HOMO in N,N'tBOCInd is further delocalized to the carbonyl arm of the substituents, stabilizing it relatively to indigo, and because the LUMO is almost unaffected, this explains the observed blueshift.

Molar extinction coefficient (ε) values (Table 1) and DFT maps of the orbital contours (see Figure 3) show that allowed π-π^* transitions are found for N,N'tBOCInd.

Spectral properties (absorption and fluorescence emission) show that while the dependence of the absorption on solvent polarity is quite small (relatively low redshift), as shown in Table 1, there is a pronounced redshift of the emission, which is also mirrored by a high Stokes shift (Δ_{SS}) in polar solvents relative to nonpolar solvents. This gains particular relevance with NtBOCInd in polar solvents with the highest Δ_{SS} value (up to ~2800 cm^{-1}).

TDDFT calculations on optimized ground (S_0) and singlet excited (S_1) electronic states carried out aiming to simulate absorption and emission, using as model solvents MCH and DMSO, representing nonpolar and polar solvents, respectively, depict Stokes shift values larger than the experimental ones but with a common trend: NtBOCInd (predicted 2726 cm^{-1} in MCH and 3242 cm^{-1} in DMSO) and with N,N'tBOCInd (predicted 1750 cm^{-1} in MCH and 2242 cm^{-1} in DMSO), see Table 1 for comparison with experimental data. Summarizing at this stage, both experimental and TDDFT calculations predict smaller Stokes shifts in *N,N'*-substituted indigos and that solvent polarity increase redshifts the emission spectra.

TDDFT-simulated absorption and emission spectra of NtBOCInd and N,N'tBOCInd (Figure SI8) match the experimentally observed spectra (Figure 2). Particularly relevant is the prediction of the second visible band at ~400 nm. Moreover, DFT calculations carried out for three possible conformations of N,N'tBOCInd, see Figure 4, show that conformer A is the only observable at room temperature being 7.5 kJ mol^{-1} more stable than conformer B. Conformer A was therefore chosen as the model compound for the subsequent studies.

With all compounds, the Stokes shift (Δ_{SS}) is reduced on going from T = 293 K to T = 77 K, which mainly results from a significant redshift of the absorption maxima (seen here as the fluorescence excitation maxima), particularly evident in indigo (Table 1).

The overall spectral changes observed at 293 and 77 K point out for a negative solvatochromism (blueshift) on going from indigo to NtBOCInd and N,N'tBOCInd (see Figure SI9 in the SI). Additional support for the above information comes from data in Table 1.

3.2.2. Photophysical Data. Fluorescence quantum yields (ϕ_F), lifetimes (τ_F), and radiative (k_F) and radiationless rate constants (k_{NR}) are given in Table 2. Observation of the photophysical parameters shows that the ϕ_F values (at 293 K) of N,N'tBOCInd are higher than those for NtBOCInd and that ϕ_F values of NtBOCInd and N,N'tBOCInd are much lower than those of indigo. Moreover, ϕ_F increases upon going from 293 to 77 K, more pronounced with N,N'tBOCInd when compared with indigo (298-fold vs 22-fold). For NtBOCInd, the fluorescence quantum yield increased 65-fold upon going from 293 to 77 K. The ϕ_F value is higher (for both NtBOCInd and N,N'tBOCInd) in the nonpolar solvents *n*-dodecane and MCH. This behavior will be further rationalized below using the TDDFT calculations.

Rate constant values in Table 2 show that the k_F values remain nearly constant in all solvents; the exception is NtBOCInd with a higher k_F value in *n*-dodecane; in contrast, nonradiative constants (k_{NR}) are found to be solvent-dependent. From Table 2, the k_{NR} values for NtBOCInd and N,N'tBOCInd are seen to be much higher than those of indigo: NtBOCInd > N,N'tBOCInd > indigo. As with indigo, in NtBOCInd and N,N'tBOCInd, the radiationless internal conversion dominates the deactivation of S_1.[54]

3.2.2.1. Deactivation Mechanisms in the Excited State for NtBOCInd and N,N'tBOCInd. The molecular mechanism behind this very efficient radiationless decay has been associated with ESPT, which may be intra or inter and imply reversible proton transfer[55,56] or it has been proposed that the relaxation of the excited C═O can be made through a

https://doi.org/10.1021/acs.jpcb.1c00120
J. Phys. Chem. B 2021, 125, 4108–4119

Table 1. Spectroscopic Properties of NtBOCInd and N,N'tBOCInd in *n*-Dodecane, MCH, 2MeTHF, EtOH, MeOH, DMF, and DMSO Solutions at T = 293 K and in 2MeTHF Solutions at T = 77 K with the Same Parameters Also Presented for Indigo in 2MeTHF, DMF, and DMSO for Comparison

compound	solvent	η[b] (cP)	ε'[c]	λ_{Abs} (nm) 293 K	λ_{Fluo} (nm) 293 K	Δ_{SS}[d] (cm^{-1}) 293 K	ε[e] 293 K	λ_{Abs} (nm) 77 K	λ_{Fluo} (nm) 77 K	Δ_{SS}[d] (cm^{-1}) 77 K
Indigo[a]	2MeTHF	0.575	7.58	602	631	763	21 424	628	638	250
	DMF	0.924	36.71	610	653	1080	22 140			
	DMSO	1.991	46.45	619	665	1117	N.D.[f]			
NtBOCInd	*n*-dodecane	1.508	2.015	554	598	1328	7248			
	MCH	0.975	2.023	553	600	1417(2726)	10 548	N.D.[f]	N.D.[f]	N.D.[f]
	2MeTHF	0.575	7.58	559	624	1863	11 162	576	615	1101
	EtOH	1.200	24.55	562	645	2290	N.D.[f]			
	MeOH	0.593	32.66	562	669	2846	N.D.[f]			
	DMF	0.924	36.71	568	651	2245	N.D.[f]			
	DMSO	1.991	46.45	574	660	2270(3242)	N.D.[f]			
N,N'tBOCInd	*n*-dodecane	1.508	2.015	548	591	1328	7927			
	MCH	0.975	2.023	547	586	1217(1750)	7122	N.D.[f]	N.D.[f]	N.D.[f]
	2MeTHF	0.575	7.58	549	597	1465	7036	561	586	760
	EtOH	1.200	24.55	549	608	1768	N.D.[f]			
	MeOH	0.593	32.66	549	610	1821	N.D.[f]			
	DMF	0.924	36.71	551	612	1809	N.D.[f]			
	DMSO	1.991	46.45	552	612	1776(2242)	N.D.[f]			

[a]For indigo, data from refs.[43,53] [b]η = Viscosity in cP.[40] [c]ε' = Dielectric constant of the solvent.[40] [d]Δ_{SS} = Stokes shift. Values in brackets predicted from TDDFT calculations. See text for further details. [e]ε = Molar absorption coefficients. [f]N.D. = Not determined.

Table 2. Photophysical Properties Including Fluorescence Quantum Yields (ϕ_F), Lifetimes (τ_F), and Rate Constants (k_F, k_{NR}) for NtBOCInd and N,N'tBOCInd in Different Organic Solvents at T = 293 K and T = 77 K with Data for Indigo for Comparison

compound	solvent	η (cP)[b]	ε'[c]	ϕ_F (77 K)	ϕ_F (293 K)	τ_F (ps)[d]	k_F (ns^{-1})[e]	k_{NR}(ns^{-1})[e]
Indigo[a]	2MeTHF	0.575	7.58	0.041	0.00190	128.1	0.015	7.79
	DMF	0.924	36.71		0.00230	135	0.017	7.39
	DMSO	1.991	46.45		0.00190	117	0.016	8.53
NtBOCInd	*n*-dodecane	1.508	2.02		0.00047	15.6	0.030	64.07
	MCH	0.975	2.02		0.00023	16.0	0.014	62.49
	2MeTHF	0.575	7.58	0.017	0.00026	21.5	0.012	46.46
	EtOH	1.200	24.55		0.00020	17.0	0.012	58.81
	MeOH	0.593	32.66		0.00012	12.4	0.01	80.64
	DMF	0.924	36.71		0.00034	19.6	0.017	51.00
	DMSO	1.991	46.45		0.00024	21.5	0.011	46.50
N,N'tBOCInd	*n*-dodecane	1.508	2.02		0.00145	108.9	0.013	9.17
	MCH	0.975	2.02		0.00117	86.1	0.014	11.61
	2MeTHF	0.575	7.58	0.155	0.00052	43.4	0.012	23.05
	EtOH	1.200	24.55		0.00030	25.4	0.012	39.31
	MeOH	0.593	32.66		0.00020	17.3	0.012	57.87
	DMF	0.924	36.71		0.00043	28.4	0.015	35.24
	DMSO	1.991	46.45		0.00054	33.9	0.016	29.48

[a]For indigo, data from refs.[43,53] [b]η = Viscosity in cP.[40] [c]ε' = Dielectric constant of the solvent.[40] [d]The decay time considered here is the slower component in the fluorescence decays. [e]$k_F = \frac{\tau_F}{\tau_F}$; $k_{NR} = \frac{1-\tau_F}{\tau_F}$.

deactivation process involving vibronic modes of the aromatic core of the molecule.[57]

The photochemistry of N,N'tBOCInd is conceptually depicted in Scheme 1.

For NtBOCInd, a first step of ballistic enolization occurs prior isomerization (Scheme 2), with TDDFT calculations showing that ESPT is nearly barrierless with the *enol* tautomer only 1 kJ mol^{-1} (MCH) above the energy of the *keto* form. This value rises to 5 kJ mol^{-1} in DMSO but is still well below the ∼11 kJ mol^{-1} observed in indigo.[43] Because the *enol* tautomer, obtained by rotation around the central carbon−carbon bond, brings the system to a conical intersection (CI), a more favorable ESPT ultimately decreases the fluorescence quantum yield and consequently also the radiative rate constant. However, this mechanism seems to be incompatible with the absence of the detected *cis* form in continuous irradiation experiments in NtBOCInd. We have recently found with related indigo systems an alternative intramolecular ESPT pathway involving pre-existing dimers,[34] not requiring a torsional movement. Moreover, the fact that no *trans*−*cis* isomerization is observed constitutes indirect evidence of the presence of dimers.

https://doi.org/10.1021/acs.jpcb.1c00120
J. Phys. Chem. B 2021, 125, 4108−4119

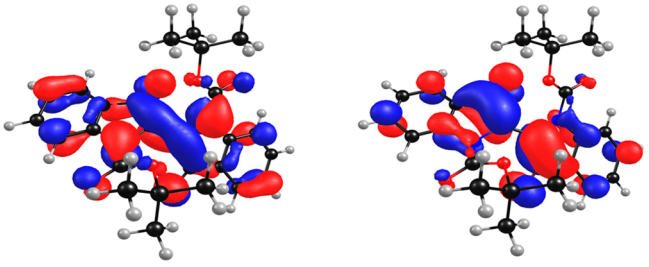

Figure 3. Orbital contours of the HOMO and LUMO in N,N'tBOCInd.

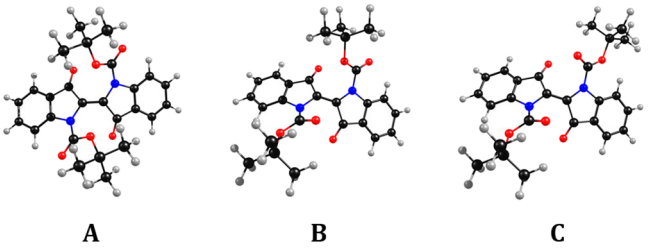

Figure 4. N,N'tBOCInd conformers (A–C). The structural differences essentially rely on the relative acyl orientation; see text for more details.

Scheme 1. Conceptual Diagram for the Behavior of N,N'tBOCInd in the Ground and First Two (S_1 and S_2) Electronic Excited States.

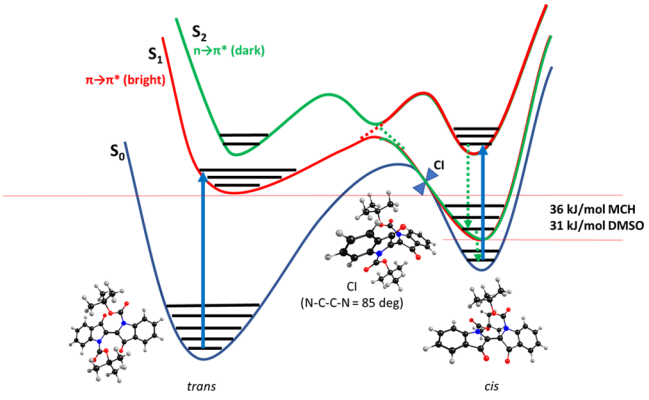

Scheme 2. Schematic Presentation of the Ballistic ESPT Reaction for NtBOCInd.

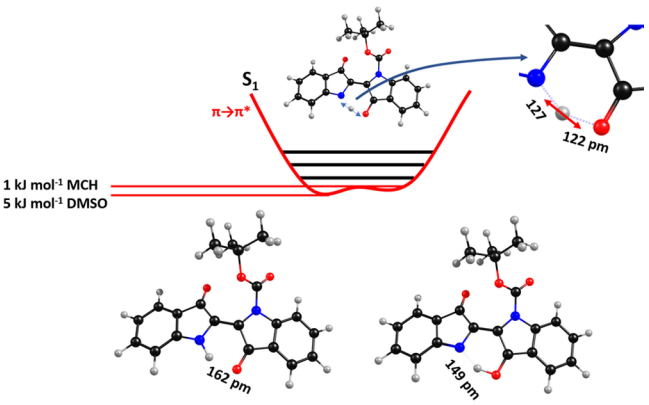

Indeed, an intramolecular ESPT would produce an *enol* tautomer, which has an emission gap of about 1.54 eV, requiring a torsional movement to reach a deactivating CI. However, an intermolecular ESPT will produce a conjugated acid/base pair A^-/AH^+ with a gap of just 0.17 eV (see the caption of Figure 5) so near the CI that it will deactivate almost instantaneously.

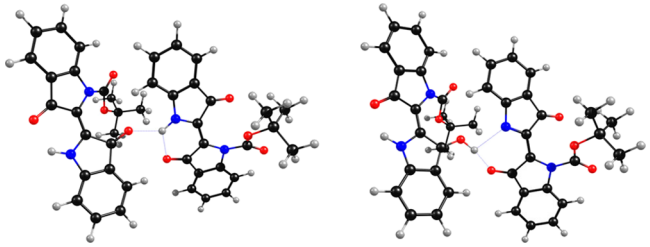

Figure 5. Proposed dimeric structures for ground (left) and excited (right) states.

Figure 5 shows the DFT- and TDDFT-optimized structures for those dimers, respectively, in the S_0 and S_1 PES. Although these values may be overestimated by basis set superposition errors (BSSEs), previously we estimated this error by the counterpoise method and provided BSSE-free values, which in the present work would scale to 32 and 29 kJ mol^{-1}, respectively, for MCH and DMSO.[34] With the dimer S_1 PES, the ESPT is downhill, and the A^-/AH^+ pair is itself near the CI, with a predicted TDDFT gap of only 0.17 eV. This pathway proposed as an alternative to the intramolecular ESPT is difficult to prove experimentally because the transients, in TA experiments, were calculated to be very similar to the ones depicted by monomers, always appearing convoluted in the experience.

With N,N'tBOCInd, the ESPT is obviously precluded; as a consequence and because the hydrogen bond N–H···O=C, anchoring the two half isatin-like moieties of indigo, is no longer present, rotation around the central carbon–carbon bond becomes available in the excited state. More relevant is that, as a consequence of this, on the S_1 surface N,N'tBOCInd is more stable in the *cis* conformation, than in the *trans*, by a surprising value of 36 kJ mol^{-1} in MCH dropping down slightly to 31 kJ mol^{-1} in DMSO (Scheme 1).

During the rotation process, the system reaches a CI, subsequently deactivating to the ground state (even in the *cis* form the gap S_0-S_1 is just 0.7 eV). As will be shown below, this precludes the back-isomerization reaction, by continuous irradiation (excitation in the *cis* form) because absorption is only allowed to S_2, which quickly deactivates to S_1. Because of the very small S_0–S_1 energy gap, internal conversion to the ground state occurs before isomerization can take place. The back-reaction is essentially thermal because in S_0 the *trans* form is the most stable. The higher yield for the back-reaction under irradiation can be explained either by a local heating, because of energy dissipation, or by activation of reactive vibrational modes in the internal conversion processes.

3.2.2.2. Time-Resolved Fluorescence. Data on the fluorescence decays for NtBOCInd and N,N'tBOCInd, summarized in Table 3, show that a single exponential properly fits the decays of the two compounds in all solvents; this clearly contrasts with indigo and other indigo derivatives.[43]

The monoexponential fluorescence decay found for NtBOCInd is likely to be associated with the decay of the

https://doi.org/10.1021/acs.jpcb.1c00120
J. Phys. Chem. B 2021, 125, 4108–4119

Table 3. Time-Resolved Fluorescence Data (Lifetimes, τ_i, Pre-Exponential Factors, a_i, and Chi-Squared Values, χ^2) Obtained with the ps-TCSPC Technique for Indigo, NtBOCInd, and N,N'tBOCInd Collected at Several Emission Wavelengths λ_{em}; λ_{exc} = 433 nm at T = 293 K

compound	λ_{exc} (nm)	solvent	λ_{em} (nm)	τ_1 (ps)	τ_2 (ps)	a_1	a_2	χ^2
indigo[a]	378	DMF	630	10.4	135	0.61	0.39	1.10
			660			−0.51	1.00	1.03
NtBOCInd	433	*n*-dodecane	590		15.6		1.00	1.26
			630				1.00	1.27
		MCH	600		16.0		1.00	1.37
			680				1.00	1.33
		2MeTHF	620		21.5		1.00	1.26
			670				1.00	1.41
		EtOH	650		17.0		1.00	1.12
			690				1.00	1.15
		MeOH	660		12.4		1.00	1.29
			690				1.00	1.32
		DMF	650		19.6		1.00	1.46
			680				1.00	1.23
		DMSO	660		21.5		1.00	1.77
			710				1.00	1.84
N,N'tBOCInd	433	*n*-dodecane	590		108.9		1.00	1.05
			650				1.00	1.29
		MCH	590		86.1		1.00	1.22
			650				1.00	1.73
		2MeTHF	610		43.4		1.00	1.47
			660				1.00	1.73
		EtOH	610		25.4		1.00	1.32
			660				1.00	1.64
		MeOH	610		17.3		1.00	1.67
			650				1.00	1.84
		DMF	610		28.4		1.00	1.52
			660				1.00	1.89
		DMSO	610		33.9		1.00	1.33
			650				1.00	1.72

[a]For indigo in DMF, data from ref.[43]

enol (tautomeric) form indicating that either (i) single proton transfer (from the *keto* form) is ultrafast (<1 ps), (ii) an unusually unstable excited-state *keto* geometry precludes ESPT, or (iii) an additional *via*, competitive with the intramolecular excited state proton transfer (InterESPT), is present; this is the case occurring when dimers (Figure 5) are present. TDDFT calculations summarized in Scheme 2 show that ESPT is nearly barrierless. In fact, if the vibrational energy is taken into account, the proton is ballistically crossing the barrier above it, mimicking the existence of a single species. The bond distance of the proton in the excited state (between the N and O atoms) of 127 and 122 pm illustrates the ballistic nature of this transfer (Scheme 2), which supports hypothesis (i) above and (iii). However, it is very interesting to observe that all the indigo-based systems that have been studied so far (including indigo itself) with intramolecular ESPT show a second longer decay time of ∼100 ps, which is absent in the NtBOCInd here investigated (Table 3).[34,36,43,53,58,59] This goes in favor of hypothesis (iii) although (i) for the reasons pointed above cannot be discarded.

For N,N'tBOCInd, the single-exponential decay is related to the most stable *cis* conformer in S_1 resulting in the rotation around the central carbon−carbon bond, with single-bond characteristics in S_1 (a 3 pm stretching value, from 136 to 139 pm). This, together with the lack of hydrogen-bonds between the N−H and C═O groups, which anchor the two half isatin-like moieties in indigo and related type molecules, leads to efficient *trans*−*cis* isomerization. As will be seen in the following section, isomerization is solvent-dependent (not observed in polar solvents) in virtue of the CI location, before the apex, in the ground-state energy profile.

3.2.3. Excited-State Isomerization (Photoisomerization) of N,N'tBOCInd in Nonpolar Solvents. Whereas in disubstituted indigo derivatives, there are several reports of *trans*−*cis* photoisomerization,[5,12,15,16,19,60,61] with monosubstituted indigo derivatives this has not been reported until very recently when Huber et al.[42] described that monoarylated indigo derivatives with relatively neutral substituents undergo *trans*−*cis* photoisomerization despite the possibility for de-excitation via ESPT.

To avoid excitation of the *cis* isomer, irradiation with monochromatic light of longer wavelength values than the absorption maxima of the *trans* isomer was performed.

Under 16 h of continuous irradiation in *n*-dodecane and MCH with a Xe lamp (150 W) at λ_{exc} = 575 nm, no changes in the UV−VIS absorption spectra are observed, indicating that photoisomerization of NtBOCInd is inhibited. In contrast, in 2MeTHF the compound showed signs of decomposition (decrease of the absorption spectra after 16 h), and once more, no *trans*−*cis* photoisomerization could be observed (Figure 6).

The above results are in line with the fact that the hydrogen bond present in NtBOCInd, responsible for the efficient ESPT

https://doi.org/10.1021/acs.jpcb.1c00120
J. Phys. Chem. B 2021, 125, 4108−4119

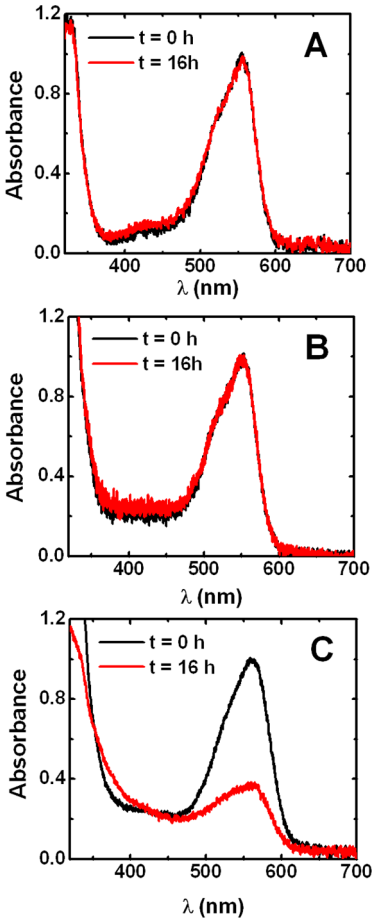

Figure 6. Absorption spectra of NtBOCInd in *n*-dodecane (A), MCH (B), and 2MeTHF(C) upon irradiation with a 150 W Xe lamp (λ_{exc} = 575 nm) for 16 h at T = 293 K.

(Scheme 2), can only be maintained in a nearly coplanar conformation of N−H···O═C (6°) or N···H−O═C (9°). Breaking this H-bonding system by rotation around the central C═C bond is energetically demanding, precluding *trans*−*cis* photoisomerization.

In the case of N,N'tBOCInd, Głowacki and co-authors showed the existence of reversible photochemical *trans*−*cis* and *cis*−*trans* isomerization with high photochemical quantum yields.[15]

Indeed, and as can be shown in Figure 7A, when N,N'tBOCInd is subjected to continuous irradiation in *n*-dodecane with λ_{exc} = 560 nm (green light), a decrease in the absorption at the maximum wavelength is observed together with the appearance of the *cis* form at ∼420 nm. Similar results were obtained in MCH and 2MeTHF, see Figure SI10A,B in the SI. It is very interesting to observe that these color changes are visible to the naked eye, see Figure 8.

In polar aprotic and polar protic solvents, *trans*−*cis* photoisomerization is inhibited, see Figure 7B and Figure SI10C-E in the SI. This is consistent with the fact that photoisomerization of indigo derivatives is precluded by intermolecular H-bonding with protic solvents.[8,62,63] In DMSO (Figure 7B) and DMF (Figure SI10E), photoisomerization is more efficiently blocked as seen by the absence of change in the absorption spectra upon irradiation.

As shown above (Scheme 1), TDDFT calculations on N,N'tBOCInd in DMSO show that, although the *cis* form can

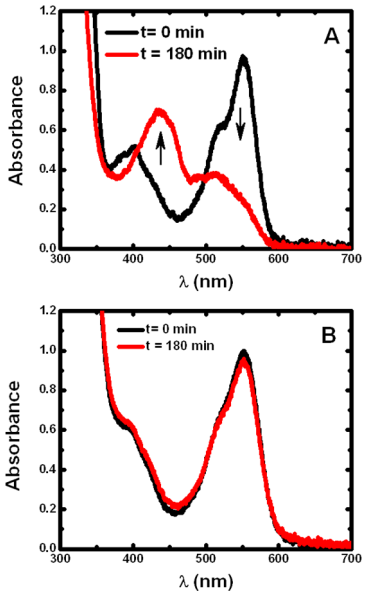

Figure 7. Absorption spectra of N,N'tBOCInd before (black) and after (red) irradiation with a 150 W xenon lamp (λ_{exc} = 560 nm) in *n*-dodecane (A) and DMSO (B) at T = 293 K. Time evolution of the spectrum is indicated by the arrows.

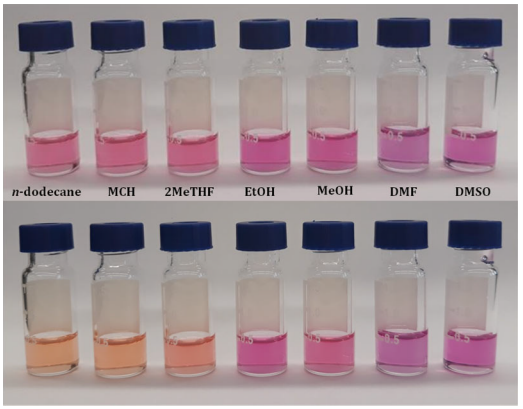

Figure 8. Picture of N,N'tBOCInd in *n*-dodecane, MCH, 2MeTHF, EtOH, MeOH, DMF, and DMSO before (top) and after (bottom) irradiation with a 150 W Xe lamp (λ_{exc} = 560 nm) at T = 293 K.

a priori be present in this solvent, the isomerization process never reaches a point in the PES that can allow it to cross the activation barrier. This is because the deactivation to S_0 is a very highly efficient process in DMSO.

A comparison of the fluorescence emission spectra obtained for N,N'tBOCInd in MCH solution before (*trans* form) and after irradiation with green light (*cis* form) showed that the emission band for the two isomers displays identical emission spectra but with a decrease in intensity (see Figure SI11 in the SI). There is no evidence for any new fluorescence bands that could be attributed to the *cis* form when 420 nm was used for the excitation (Figure SI11, black line), and TDDFT also predicts the absence of fluorescence because of the nature of the S_1 state (n,π^*). Similar behavior was observed in *n*-dodecane and 2MeTHF (Table 4), indicating that only the *trans* isomer of N,N'tBOCInd displays fluorescence.

To further help answering the question of whether *trans* to *cis* photoisomerization can occur, in the excite state, the fluorescence decays of N,N'tBOCInd, obtained after irradi-

https://doi.org/10.1021/acs.jpcb.1c00120
J. Phys. Chem. B 2021, 125, 4108−4119

Table 4. Absorption and Fluorescence Emission Data for the *cis* Isomer of N,N'tBOCInd in *n*-Dodecane, MCH, and 2MeTHF at T = 293 K

compound	solvent	η^a	ε'^b	λ_{Abs} (nm)	λ_{Fluo} (nm)
cis N,N'tBOCInd	*n*-dodecane	1.508	2.015	422/509	591 (591)[c]
	MCH	0.975	2.023	421/511	586 (586)[c]
	2MeTHF	0.575	7.580	421/513	597 (597)[c]

[a]η = Viscosity in cP.[40] [b]ε' = Dielectric constant of the solvent.[40] [c]Fluorescence emission values, λ_{Fluo}, from the *trans* isomer in parentheses.

ation with green light, were obtained in MCH (see Figure SI12). If coexistence of both isomers in the excited state exists (and if these are both emissive), it would be expected that they will present different decay times. This is not what is observed in the time-resolved experiments (Figure SI12). Indeed, with the very close similarities of the observed decay times before (86 ps) and after (92 ps) irradiation, it is possible to conclude that only the *trans* is emissive from S_1.

3.2.3.1. Thermal Reversible Isomerization and cis−trans Photoisomerization of N,N'tBOCInd. The occurrence of thermal (dark) reversible isomerization, concomitant with a photochemical *cis−trans* isomerization process, was investigated, in several solvents, by measuring the absorption of one sample kept in the dark (Figure 9).

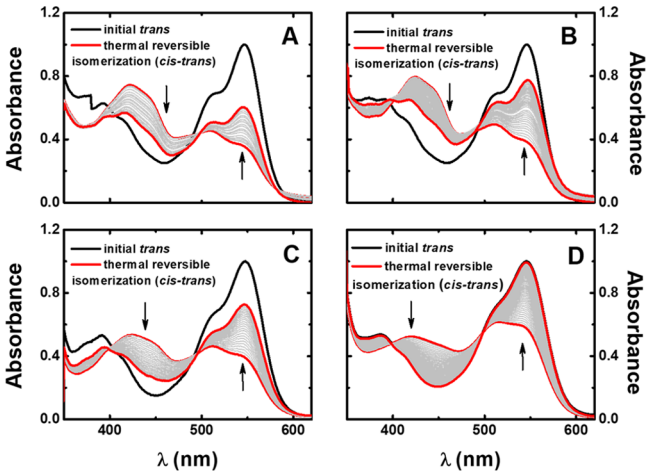

Figure 9. Thermal *cis−trans* recovery of N,N'tBOCInd in *n*-dodecane (A), MCH (B), 2MeTHF (C), and MeCN(D) at T = 293 K. The black lines show the initial *trans N,N'*tBOCInd, and time evolution of the spectrum is indicated by the arrows.

The results showed that in the *cis−trans* thermal relaxation of N,N'tBOCInd only partial recovery of the original absorption is observed. Comparing these results with previously reported data for N,N'tBOCInd in MeCN,[15] where the process was completely reversible and the original absorption was obtained, the current data show that for N,N'tBOCInd reversible thermal relaxation is solvent-dependent.

The rate constants for the thermal *cis−trans* isomerization reaction were further obtained following a first-order kinetic law for the isomerization process,[64] according to eq 3,

$$\ln \frac{A_t - A_\infty}{A_0 - A_\infty} = -k_\Delta t \tag{3}$$

where A_0 corresponds to the initial absorbance (at the beginning of the dark reversion), A_t is the absorbance measured during the isomerization process, and A_∞ is the absorbance after the equilibrium. The values of A_0, A_t, and A_∞ were measured at the wavelength maxima of each solvent (λ_{Abs}^{max}). Figure SI13 shows the plots (eq 3) from where the rate constants k_Δ (thermal *cis−trans* isomerization) could be obtained. It is seen that k_Δ is higher in solvents with lower viscosity. These results clearly show that the kinetics of the thermal *cis−trans* isomerization reaction of N,N'tBOCInd is strongly dependent on the solvent's viscosity.

3.2.3.2. Trans−cis and cis−trans Photoisomerization Quantum Yields. To quantitatively evaluate the efficiency of the photochemical processes, reaction quantum yields were obtained. These are most favorably obtained when the incident light is monochromatic.[40] The quantum yields of photoisomerization were obtained with the setup illustrated in Figure SI14.

The rate of *trans−cis* (λ_{exc} = 560 nm) and *cis−trans* (λ_{exc} = 416 nm) photoisomerization follows a first-order kinetic law and was further calculated from eq 4,[15]

$$\frac{\phi_{i\rightarrow j}}{V} = -\left(\frac{\frac{\delta_c}{\delta_t}}{I_{abs}}\right)_{t=0} \tag{4}$$

where $\phi_{i\rightarrow j}$ stands for the quantum yield of *trans−cis* or *cis−trans* isomerization, V is the final volume of the solution, the ratio $\frac{\delta_c}{\delta_t}$ is obtained from the slope of the plot of the concentration (c) versus the irradiation time (t), and I_{abs} are the moles of photons absorbed by the irradiated solution per second (einstein s^{-1}).

Trans−cis ($\phi_{trans-cis}$) and *cis−trans* ($\phi_{cis-trans}$) photoisomerization quantum yields, obtained in various solvents (varying the polarity and viscosity), are presented in Table 5 (for further details please see Figure SI15−22 in the SI).

Table 5. Quantum Yields for *trans−cis* and *cis−trans* Photoisomerization of N,N'tBOCInd in *n*-Dodecane, MCH, 2MeTHF, and MeCN at T = 293 K

solvent	η (cP)[a]	ε'^b	$\phi_{trans-cis}$	$\phi_{cis-trans}$
n-dodecane	1.508	2.02	0.15	0.04
MCH	0.975	2.02	0.39	0.16
2MeTHF	0.575	7.58	0.24	0.14
MeCN	0.345	35.9	0.11	0.43

[a]η = Viscosity in cP.[40] [b]ε' = Dielectric constant of the solvent.[40]

As with the other excited-state deactivation pathways (photophysical processes), photoisomerization quantum yields (photochemical processes) are also solvent-dependent. The values of the photoisomerization quantum yields in MeCN ($\phi_{trans-cis}$ = 0.11 and $\phi_{cis-trans}$ = 0.43) are in excellent agreement with previously reported values ($\phi_{trans-cis}$ = 0.13 and $\phi_{cis-trans}$ = 0.46) in ref.[15] Observation of data in Table 5 indicates that while *trans−cis* isomerization quantum yields do

https://doi.org/10.1021/acs.jpcb.1c00120
J. Phys. Chem. B 2021, 125, 4108−4119

not depend on solvent viscosity or polarity, *cis*−*trans* isomerization quantum yields are found to be viscosity-dependent, with higher values in MeCN (η = 0.345 cP) and lower values in *n*-dodecane (η = 1.508 cP). Moreover, it is also seen that *cis* N,N'tBOCInd isomerizes to *trans* with much lower efficiencies than those for the *trans*−*cis* isomerization in all solvents, with the exception of MeCN.

4. CONCLUSIONS

Two *tert*-butoxy carbonyl indigo derivatives, NtBOCInd and N,N'tBOCInd, were synthesized with a new synthetic methodology with favorable green chemistry metrics indicating that the new strategy is favorable regarding the impact of chemical processes on the environment. Different decay pathways are observed for the two *tert*-butoxy carbonyl indigo derivatives. With NtBOCInd, photoisomerization was found absent, whereas with N,N'tBOCInd photoisomerization was found to be present in nonpolar solvents and absent in protic polar solvents. The absence of other deactivation processes with NtBOCInd, including photoisomerization, is attributed to a ballistic ESPT in this compound, which is justified from the single exponential nature of the decay and from TDDFT calculations. Excitation with green/blue light of N,N'tBOCInd leads to solvent-dependent *trans*−*cis*/*cis*−*trans* photoisomerization with quantum yields $\phi_{trans-cis}$ =0.11−0.30 and $\phi_{cis-trans}$ = 0.04−0.43. Reversible *cis*−*trans* isomerization can also be observed by thermal (dark) deactivation with rate constant values for this process found to be solvent viscosity-dependent. A larger radiative contribution (reflected in high lifetime values, fluorescent quantum yields, and radiative rate constants) is observed in nonpolar when compared to polar solvents. This is found to be because of a smaller S_0 - S_1 PES gap, which, in polar solvents, reaches zero—the CI—before the climax of the ground state path, while in nonpolar solvents, it deactivates after the apex in the ground state *cis*−*trans* pathway. The CI location is found to depend on the $\pi,\pi^*/n,\pi^*$ crossing, which occurs sooner in polar solvents because of a higher stabilization of the dark n,π^* state.

■ ASSOCIATED CONTENT

Supporting Information

The Supporting Information is available free of charge at https://pubs.acs.org/doi/10.1021/acs.jpcb.1c00120.

Schematic of MW-assisted synthesis of NtBOCInd and N,N'tBOCInd from indigo, ^{1}H NMR of NtBOCInd in $CDCl_3$, ^{13}C NMR of NtBOCInd in CDCl3, ^{1}H NMR of N,N'tBOCInd in $CDCl_3$, ^{13}C NMR of N,N'tBOCInd in $CDCl_3$, high-resolution mass spectrum of NtBOCInd, high-resolution mass spectrum of N,N'tBOCInd, orbital contours of the HOMO and LUMO in indigo, TDDFT-simulated spectra of NtBOCInd and N,N'tBOCInd in MCH and DMSO, normalized absorption and fluorescence emission spectra, absorption spectra of N,N'tBOCInd before and after irradiation, fluorescence emission spectra of *trans* and *cis* isomers of N,N'tBOCInd in MCH, fluorescence decay and pulse instrumental response obtained for N,N'tBOCInd, determination of the rate constants, schematic representation of the experimental setup and picture of the irradiation system, and absorption spectra for *trans*−*cis* isomerization of N,N'tBOCInd in n-dodecane, MCH, 2MeTHF, and MeCN (PDF)

■ AUTHOR INFORMATION

Corresponding Author

J. Sérgio Seixas de Melo − *University of Coimbra, CQC, Department of Chemistry, 3004-535 Coimbra, Portugal;* orcid.org/0000-0001-9708-5079; Email: sseixas@ci.uc.pt

Authors

Daniela Pinheiro − *University of Coimbra, CQC, Department of Chemistry, 3004-535 Coimbra, Portugal*

Adelino M. Galvão − *Centro de Química Estrutural, Departamento de Engenharia Química, Instituto Superior Técnico (IST), Universidade de Lisboa, 1049-001 Lisboa, Portugal*

Marta Pineiro − *University of Coimbra, CQC, Department of Chemistry, 3004-535 Coimbra, Portugal;* orcid.org/0000-0002-7460-3758

Complete contact information is available at: https://pubs.acs.org/10.1021/acs.jpcb.1c00120

Notes

The authors declare no competing financial interest.

■ ACKNOWLEDGMENTS

This work was supported by Project "Hylight" (no. 031625) 02/SAICT/2017, PTDC/QUI-QFI/31625/2017, which is funded by the Portuguese Science Foundation and Compete Centro 2020, Project Suprasol (LISBOA-01-0145-FEDER-028365 − PTDC/QUI-QOR/28365/2017), funded by Fundo Europeu de Desenvolvimento Regional (FEDER), through Programa Operacional Regional LISBOA (LISBOA2020), financially supported by project "SunStorage - Harvesting and storage of solar energy" reference POCI-01-0145-FEDER-016387, funded by FEDER, through Programa Operacional Factores de Competitividade (COMPETE) 2020 - Operational Programme for Competitiveness and Internationalization (OPCI), and by national funds, through Fundação para a Ciência e a Tecnologia (FCT), the Portuguese Agency for Scientific Research. We also acknowledge funding by FEDER through COMPETE. The Coimbra Chemistry Centre is supported by the FCT, through Projects UIDB/00313/2020 and UIDP/00313/2020, and CQE is supported by the FCT through project UID/QUI/00100/2019. The FCT is also gratefully acknowledged for a PhD grant to D. Pinheiro (ref SFRH/BD/74351/2010). D. Pinheiro also acknowledges the project "SunStorage - Harvesting and storage of solar energy" for a research grant.

■ REFERENCES

(1) Koeppe, B.; Schröder, V. R. F. Effects of Polar Substituents and Media on the Performance of *N,N′*-Di-Tert-Butoxycarbonyl-Indigos as Photoswitches. *ChemPhotoChem* **2019**, *3*, 1−7.

(2) Petermayer, C.; Dube, H. Indigoid Photoswitches: Visible Light Responsive Molecular Tools. *Acc. Chem. Res.* **2018**, *51*, 1153−1163.

(3) Huang, C.-Y.; Bonasera, A.; Hristov, L.; Garmshausen, Y.; Schmidt, B. M.; Jacquemin, D.; Hecht, S. *N,N′*-Disubstituted Indigos as Readily Available Red-Light Photoswitches with Tunable Thermal Half-Lives. *J. Am. Chem. Soc.* **2017**, *139*, 15205−15211.

(4) Crano, J. C.; Guglielmetti, R. J., *Organic Photochromic and Thermochromic Compounds: Photochromic Families*; Kluwer Academic Publishers: New York, Boston, Dordrecht, London, Moscow, 1999.

(5) Brode, W. R.; Pearson, E. G.; Wyman, G. M. The Relation between the Absorption Spectra and the Chemical Constitution of

Dyes. Xxvii. *Cis-Trans* Isomerism and Hydrogen Bonding in Indigo Dyes. *J. Am. Chem. Soc.* **1954**, *76*, 1034−1036.
(6) Pereira, R. C.; Pineiro, M.; Galvão, A. M.; Seixas de Melo, J. S. Thioindigo, and Sulfonated Thioindigo Derivatives as Solvent Polarity Dependent Fluorescent on-Off Systems. *Dyes Pigm.* **2018**, *158*, 259−266.
(7) Dittmann, M.; Graupner, F. F.; Maerz, B.; Oesterling, S.; de Vivie-Riedle, R.; Zinth, W.; Engelhard, M.; Lüttke, W. Photostability of 4,4′-Dihydroxythioindigo, a Mimetic of Indigo. *Angew. Chem., Int. Ed.* **2014**, *53*, 591−594.
(8) Rogers, D. A.; Margerum, J. D.; Wyman, G. M. Spectroscopic Studies on Dyes. Iv. The Fluorescence Spectra of Thioindigo Dyes. *J. Am. Chem. Soc.* **1957**, *79*, 2464−2468.
(9) Wyman, G. M.; Brode, W. R. The Relation between the Absorption Spectra and the Chemical Constitution of Dyes Xxii. *Cis-Trans* Isomerism in Thioindigo Dyes. *J. Am. Chem. Soc.* **1951**, *73*, 1487−1493.
(10) Güsten, H. Photochemical *Cis*−*Trans*-Isomerization of Trans-Bis-2,2′-(3-Oxo-2,3-Dihydrobenzo[B]Furylidine)(Oxindigo). *Chem. Commun.* **1969**, 133b−1134b.
(11) Wyman, G. M.; Zarnegar, B. M. Excited State Chemistry of Indigoid Dyes. I. Fluorescence Versus *Cis-Trans* Isomerization. *J. Phys. Chem.* **1973**, *77*, 831−837.
(12) Ross, D. L.; Blanc, J.; Matticoli, F. J. Photochromic Indigoids. Ii. Absorption Spectra and Quantum Yields for the Photoisomerization of Selenoindigo. *J. Am. Chem. Soc.* **1970**, *92*, 5750−5752.
(13) Nobre, D. C.; Cunha, C.; Porciello, A.; Valentini, F.; Marrocchi, A.; Vaccaro, L.; Galvão, A. M.; Seixas de Melo, J. S. Photoresponsive N,N′-Disubstituted Indigo Derivatives. *Dyes Pigm.* **2020**, *176*, No. 108197.
(14) Nakagawa, H.; Matsumoto, A.; Daicho, A.; Ozaki, Y.; Ota, C.; Nagasawa, Y. Solvent Dependent *Trans - Cis* Photoisomerization of *N,N′*-Diacetylindigo Studied by Femtosecond Time-Resolved Transient Absorption Spectroscopy. *J. Photochem. Photobiol. A* **2018**, *358*, 308−314.
(15) Farka, D.; Scharber, M.; Glowacki, E. D.; Sariciftci, N. S. Reversible Photochemical Isomerization of *N,N′*-Di(T-Butoxycarbonyl)Indigos. *J. Phys. Chem. A* **2015**, *119*, 3563−3568.
(16) Nicholls-Allison, E. C.; Nawn, G.; Patrick, B. O.; Hicks, R. G. Protoisomerization of Indigo Di- and Monoimines. *Chem. Commun.* **2015**, *51*, 12482−12485.
(17) Görner, H.; Schulte-Frohlinde, D. Laser Flash Studies of Thioindigo and Indigo Dyes. Evidence for a *Trans* Configuration of the Triplet State. *Chem. Phys. Lett.* **1979**, *66*, 363−369.
(18) Blanc, J.; Ross, D. L. Procedure for Determining the Absorption Spectra of Mixed Photochromic Isomers Not Requiring Their Separation. *J. Phys. Chem.* **1968**, *72*, 2817−2824.
(19) Giuliano, C.; Hess, L.; Margerum, J. *Cis-Trans* Isomerization and Pulsed Laser Studies of Substituted Indigo Dyes. *J. Am. Chem. Soc.* **1968**, *90*, 587−594.
(20) Alphen, J. V. The Colour of N,N′-Diethylindigo (on Indigo Vii). *Recl. Trav. Chim. Pays-Bas* **1942**, *61*, 201−208.
(21) Rondão, R.; Seixas de Melo, J. S.; Melo, M. J.; Parola, A. J. Excited-State Isomerization of Leuco Indigo. *J. Phys. Chem. A* **2012**, *116*, 2826−2832.
(22) Glowacki, E. D.; Voss, G.; Sariciftci, N. S. 25th Anniversary Article: Progress in Chemistry and Applications of Functional Indigos for Organic Electronics. *Adv. Mater.* **2013**, *25*, 6783−6800.
(23) Glowacki, E. D.; Voss, G.; Demirak, K.; Havlicek, M.; Sunger, N.; Okur, A. C.; Monkowius, U.; Gasiorowski, J.; Leonat, L.; Sariciftci, N. S. A Facile Protection-Deprotection Route for Obtaining Indigo Pigments as Thin Films and Their Applications in Organic Bulk Heterojunctions. *Chem. Comm.* **2013**, *49*, 6063−6065.
(24) Pina, F.; Hatton, T. A. Photochromic Soft Materials: Flavylium Compounds Incorporated into Pluronic F-127 Hydrogel Matrixes. *Langmuir* **2008**, *24*, 2356−2364.
(25) Evans, R. A.; Hanley, T. L.; Skidmore, M. A.; Davis, T. P.; Such, G. K.; Yee, L. H.; Ball, G. E.; Lewis, D. A. The Generic Enhancement of Photochromic Dye Switching Speeds in a Rigid Polymer Matrix. *Nat. Mater.* **2005**, *4*, 249−253.
(26) Crano, J. C.; Flood, T.; Knowles, D.; Kumar, A.; Van Gemert, B. Photochromic Compounds: Chemistry and Application in Ophthalmic Lenses. *pac* **1996**, *68*, 1395−1398.
(27) Ikeda, T.; Tsutsumi, O.; Wu, Y. Optical Switching and Image Storage by Means of Photochromic Liquid Crystals. *Mol. Cryst. and Liq. Cryst.* **2000**, *347*, 1−13.
(28) Glowacki, E.; Horovitz, K.; Tang, C. W.; Marshall, K. L. Photoswitchable Gas Permeation Membranes Based on Liquid Crystals. *Adv. Funct. Mater.* **2010**, *20*, 2778−2785.
(29) Lerch, M. M.; Hansen, M. J.; van Dam, G. M.; Szymanski, W.; Feringa, B. L. Emerging Targets in Photopharmacology. *Angew. Chem., Int. Ed.* **2016**, *55*, 10978−10999.
(30) Broichhagen, J.; Frank, J. A.; Trauner, D. A Roadmap to Success in Photopharmacology. *Acc. Chem. Res.* **2015**, *48*, 1947−1960.
(31) Velema, W. A.; Szymanski, W.; Feringa, B. L. Photopharmacology: Beyond Proof of Principle. *J. Am. Chem. Soc.* **2014**, *136*, 2178−2191.
(32) Heilemann, M.; Dedecker, P.; Hofkens, J.; Sauer, M. Photoswitches: Key Molecules for Subdiffraction-Resolution Fluorescence Imaging and Molecular Quantification. *Laser & Photon. Rev.* **2009**, *3*, 180−202.
(33) Fehrentz, T.; Schönberger, M.; Trauner, D. Optochemical Genetics. *Angew. Chem., Int. Ed.* **2011**, *50*, 12156−12182.
(34) Pinheiro, D.; Pineiro, M.; Galvão, A. M.; Seixas de Melo, J. S. Deep in Blue with Green Chemistry: Influence of Solvent and Chain Length on the Behaviour of N- and N,N′- Alkyl Indigo Derivatives. *Chem. Sci.* **2021**, *12*, 303−313.
(35) Seixas de Melo, J. S., The Molecules of Colour and Art. Molecules with History and Modern Applications. In *Photochemistry*; Albini, A.; Prodi, S., Eds. The Royal Society of Chemistry: London, 2020; *47*, 196−216.
(36) Seixas de Melo, J. S.; Rondão, R.; Burrows, H. D.; Melo, M. J.; Navaratnam, S.; Edge, R.; Voss, G. Spectral and Photophysical Studies of Substituted Indigo Derivatives in Their Keto Forms. *ChemPhysChem* **2006**, *7*, 2303−2311.
(37) Murov, S.; Carmichael, I.; Hug, G., *Handbook of Photochemistry*, 2nd Edition ed.; CRC Press: New York, 1993.
(38) Pina, J.; Seixas de Melo, J. S.; Burrows, H. D.; Maçanita, A. L.; Galbrecht, F.; Bünnagel, T.; Scherf, U. Alternating Binaphthyl−Thiophene Copolymers: Synthesis, Spectroscopy, and Photophysics and Their Relevance to the Question of Energy Migration Versus Conformational Relaxation. *Macromolecules* **2009**, *42*, 1710−1719.
(39) Striker, G.; Subramaniam, V.; Seidel, C. A. M.; Volkmer, A. Photochromicity and Fluorescence Lifetimes of Green Fluorescent Protein. *J. Phys. Chem. B* **1999**, *103*, 8612−8617.
(40) Montalti, M.; Credi, A.; Prodi, L.; Gandolfi, M. T., *Handbook of Photochemistry*, 3rd Edition ed.; Taylor & Francis Group, LLC: Boca Raton, 2006.
(41) Schmidt, M. W.; et al. General Atomic and Molecular Electronic Structure System. *J. Comput. Chem.* **1993**, *14*, 1347−1363.
(42) Huber, L. A.; Mayer, P.; Dube, H. Photoisomerization of Mono-Arylated Indigo and Water-Induced Acceleration of Thermal Cis-to-Trans Isomerization. *ChemPhotoChem* **2018**, *2*, 458−464.
(43) Pina, J.; Sarmento, D.; Accoto, M.; Gentili, P. L.; Vaccaro, L.; Galvão, A. M.; Seixas de Melo, J. S. Excited-State Proton Transfer in Indigo. *J. Phys. Chem. B* **2017**, *121*, 2308−2318.
(44) Shakoori, A.; Bremner, J. B.; Abdel-Hamid, M. K.; Willis, A. C.; Haritakun, R.; Keller, P. A. Further Exploration of the Heterocyclic Diversity Accessible from the Allylation Chemistry of Indigo. *Beilstein J. Org. Chem.* **2015**, *11*, 481−492.
(45) Sheldon, R. A. The E Factor 25 Years On: The Rise of Green Chemistry and Sustainability. *Green Chem.* **2017**, *19*, 18−43.
(46) Ichimura, K.; Arimitsu, K.; Tahara, M. Photoacid-Catalysed Pigmentation of Dyestuff Precursors Enhanced by Acid Amplifiers in Polymer Films. *J. Mater. Chem.* **2004**, *14*, 1164−1172.

https://doi.org/10.1021/acs.jpcb.1c00120
J. Phys. Chem. B 2021, 125, 4108−4119

(47) Sheldon, R. A. Metrics of Green Chemistry and Sustainability: Past, Present, and Future. *ACS Sustainable Chem. Eng.* **2018**, *6*, 32−48.
(48) Van Aken, K.; Strekowski, L.; Patiny, L. Ecoscale, a Semi-Quantitative Tool to Select an Organic Preparation Based on Economical and Ecological Parameters. *Beilstein J. Org. Chem.* **2006**, *2*, 3.
(49) Seixas de Melo, J. S., The Molecules of Colour. In *Photochemistry*, Albini, A.; Fasani, E.; Protti, S., Eds. The Royal Society of Chemistry: London, 2018; *45*, 68−100.
(50) Klessinger, M. The Origin of the Colour of Indigo Dyes. *Dyes Pigm.* **1982**, *3*, 235−241.
(51) Lüttke, W.; Hermann, H.; Klessinger, M. Theoretically and Experimentally Determined Properties of the Fundamental Indigo Chromophore. *Angew. Chem., Int. Ed.* **1966**, *5*, 598−599.
(52) Sadler, P. W. Absorption Spectra of Indigoid Dyes. *J. Org. Chem.* **1956**, *21*, 316−318.
(53) Seixas de Melo, J. S.; Moura, A. P.; Melo, M. J. Photophysical and Spectroscopic Studies of Indigo Derivatives in Their Keto and Leuco Forms. *J. Phys. Chem. A* **2004**, *108*, 6975−6981.
(54) Seixas de Melo, J. S.; Burrows, H. D.; Serpa, C.; Arnaut, L. G. The Triplet State of Indigo. *Angew. Chem., Int. Ed.* **2007**, *46*, 2094−2096.
(55) Iwakura, I.; Yabushita, A.; Kobayashi, T. Why Is Indigo Photostable over Extremely Long Periods? *Chem. Lett.* **2009**, *38*, 1020−1021.
(56) He, X.; Yang, F.; Li, S.; He, X.; Yu, A.; Chen, J.; Xu, J.; Wang, J. Ultrafast Excited-State Intermolecular Proton Transfer in Indigo Oligomer. *J. Phys. Chem. A* **2019**, *123*, 6463−6471.
(57) He, X.; Yu, P.; Zhao, J.; Wang, J. Efficient Vibrational Energy Transfer through Covalent Bond in Indigo Carmine Revealed by Nonlinear Ir Spectroscopy. *J. Phys. Chem. B* **2017**, *121*, 9411−9421.
(58) Rondão, R. J.; Seixas de Melo, J. S.; Schaberle, F. B.; Voss, G. Excited State Characterization of a Polymeric Indigo. *Phys. Chem. Chem. Phys.* **2012**, *14*, 1778−1783.
(59) Seixas de Melo, J.; Rondão, R.; Burrows, H. D.; Melo, M. J.; Navaratnam, S.; Edge, R.; Voss, G. Photophysics of an Indigo Derivative (Keto and Leuco Structures) with Singular Properties. *J. Phys. Chem. A* **2006**, *110*, 13653−13661.
(60) Görner, H.; Pouliquen, J.; Kossanyi, J. Trans to Cis Photoisomerization of N,N′-Disubstituted Indigo Dyes Via Excited Singlet States; a Laser Flash Photolysis and Steady State Irradiation Study. *Can. J. Chem.* **1987**, *65*, 708−717.
(61) Wyman, G. M.; Zenhäusern, A. F. Spectroscopic Studies on Dyes V. Derivatives of Cis-Indigo. *J. Org. Chem.* **1965**, *30*, 2348−2352.
(62) Schneider, S.; Lill, E.; Hefferle, P.; Dörr, F. Influence of Intramolecular and Intermolecular Hydrogen Bonding on the Fluorescence Decay Time of Indigo Derivatives. *Il Nuovo Cimento* **1981**, *63B*, 411−419.
(63) Windhager, W.; Schneider, S.; Dörr, F. On the Influence of Intra - and Inter-Molecular Hydrogen Bonding on the Excited State Lifetime of Indigo Dyes. *zna* **1977**, *32*, 876−878.
(64) Miniewicz, A.; Orlikowska, H.; Sobolewska, A.; Bartkiewicz, S. Kinetics of Thermal *Cis*−*Trans* Isomerization in a Phototropic Azobenzene-Based Single-Component Liquid Crystal in Its Nematic and Isotropic Phases. *Phys. Chem. Chem. Phys.* **2018**, *20*, 2904−2913.

https://doi.org/10.1021/acs.jpcb.1c00120
J. Phys. Chem. B 2021, 125, 4108−4119